A Dedicated Dual Energy X-ray Tomography/Radiography Equipment on-board of R/V *Mare Nigrum*

Mihai Iovea [1], Marian Neagu [1], Octavian G. Duliu [2],
Gheorghe Oaie [3], Gabriela Mateiasi [4]

[1] Accent Pro 2000, Ltd, 1, Nerva Traian Str., K6, 031041, Bucharest, Romania,
phone: +4074 518 2660, e-mali: miovea@pcnet.ro
[2] University of Bucharest, Department of Atomic and Nuclear Physics, P.O. Box MG-11,
077125 Bucharest, Romania, e-mail: duliu@b.astral.ro
[3] National Institute of Marine Geology and Geoecology, 23-25 Dimitrie Onciu Str.,
024504, Bucharet, Romania, e-mail: goaie@geoecomar.ro
[4] The Politehnica University, Bucharest, 313, Splaiul Independentei, 060032, Bucharest, Romania,
e-mail: miovea@pcnet.ro

Abstract

An X-ray dual-energy computer tomograph provided with a double set of X-ray detectors arrays separated by a copper foil was projected, assembled and commissioned to be used on-board of the R/V Mare Nigrum. By using a variant of filtered back projections reconstruction algorithm together with a set of calibrated standard samples, it was possible do determine on-board and with a precision of 3.5 % the density and 2.5 % the effective atomic number distribution of various unconsolidated sediments core. The same computer tomograph was used to obtain free of parallax dual energy digital radiography, allowing a spatial resolution of about 0.5 mm.

Keywords: Dual-energy computed tomography, dual-energy digital radiography, unconsolidated sediments, effective atomic number, on-board, R/V Mare Nigrum

1. Introduction

Digital Radiography (DR) and in particular Computed Tomography (CT) represent the ultimate development of the oldest method of non-invasive control and, at the same time, the first large scale application high energy ionizing radiation. The progress of both methods was significantly facilitated by a rapid evolution of numerical methods as well as computing techniques together with the creation of new and more sensitive and stable detection systems for X and gamma-rays and, at some extent, for neutrons.

Although, in 1972, the first full operational Computer Tomograph (CtT) was designed for medical diagnosis [1] in less than 10 years CT begun to be intensively applied in other branches of scientific investigation such as palaeontology [2], soil science [2], petroleum science [3], petrology [4,5], sedimentology [6], mineralogy [7] or non-destructive industrial control [8-10].

At their passages through matter monochromatic X or gamma-rays are attenuated following well known Lambert-Bougé law:

$$I = I_0\, e^{-\int \mu(x,y,z)dr} \tag{1}$$

where: *I* represents the intensity of transmitted current of photons, I_0 is the intensity of incident current of photons, $\mu(x,y,z)$ represents the Linear Attenuation Coefficient (LAC) function of the object, which for inhomogeneous samples takes different values for different points of the considered object.

At its turn, LAC depends in a rather complex manner on both density and effective atomic number (Z_{eff}) of the absorber. For that reason, from the point of view of the
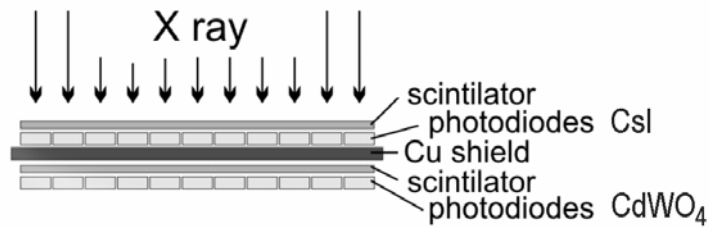
Figure 1. The experimental set-up of detectors used in the case of DE-CT

interaction with gamma of X-rays, any object can be described by means of a 3D function of its LAC.

Further, depending on the detection system used for transmitted radiation, both 2D projections and 2D reconstructions of the LAC could be obtained. In the case of a flat, mosaic-like and immobile system of microscopic detectors it results a radiograph (analogue or digital) of the object. If by contrary, the object rotates itself by respect to radiation source and detectors (flat panel of diode array or other kind of solid state detectors), from the multitude of different projections of the LAC of the object, after a complex data processing the LAC function of a section or of the entire volume of the investigated object is digitally reconstructed, resulting in this way a 2D or a 3D tomography of the object [11-15].

It is worth to mention that the LAC of any material or element represents the product between density ρ and the mass attenuation coefficient (MAC), the last one depending only on Z_{eff} and X- or gamma ray energy. On the other hand, MAC contains two terms, the first describing the photoelectric effect, important for energies below 100 keV and low atomic numbers while the second term accounts for Compton inelastic scattering that is predominant for energies higher than 100–200 keV. In the case of heavier elements such as iron, copper or lead, the LAC depends less or more on the atomic number even for higher than 200 keV energies [16].

As a result, for mineral samples containing both low and high atomic number elements, the only quantitative information that can be inferred by analyzing CT images mainly referees to the local valued of LAC, which, in some cases could be insufficient for a more detailed analysis.

This inconveniency was significantly overcome by using a dual-energy CT (DE-CT) [17-21] that, by measuring the same section through investigated sample by means of two X- or gamma rays having different energies it was possible to determine the local values of both density and Z_{eff} of the chosen section. One of the best ways to accomplish this task consists of using a single X-ray generator and a set of two solid-sate detectors separated by a thin, 1 mm copper shield that considerably modifies the spectral composition of the radiation detected by each set of detectors. Coupled with an appropriate collection of standard samples with well known densities and atomic numbers, and by using suitable reconstruction algorithms, two different CAT images of the same sections are finally computed, one of them representing local densities and the other one the distribution of the Z_{eff}.

In addition to generate, CT images, any CtT can be successfully used to obtain high resolution digital radiographs by translating the object between X-ray tube and detectors. This variant of DR, firstly used by Algeo et al. [22] to investigate sedimentary cores provides high resolution images completely free of parallax error as the field of
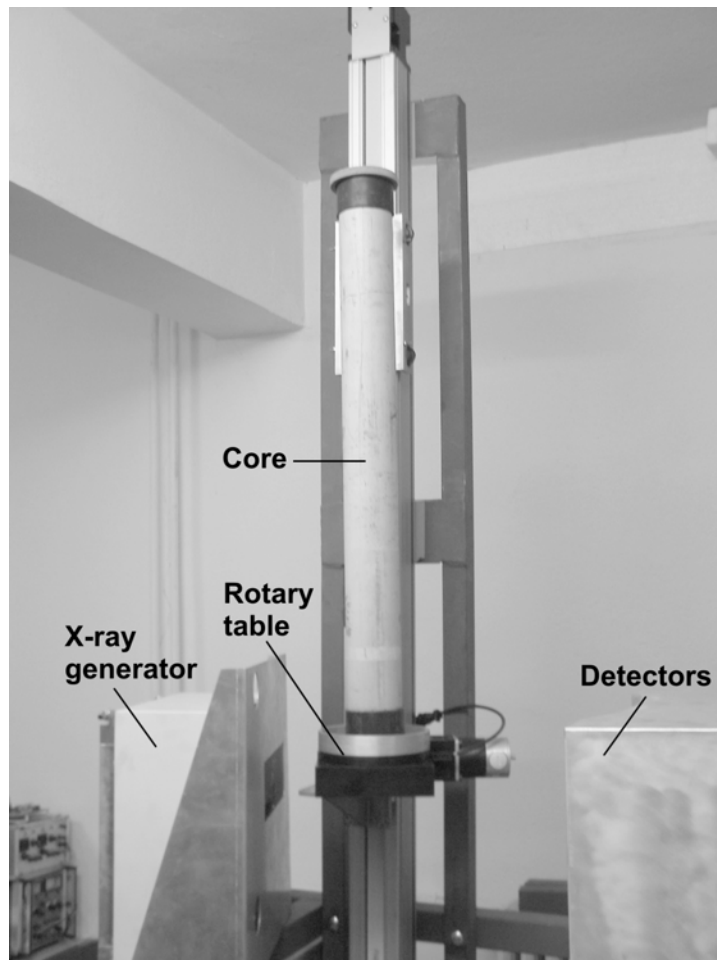
Figure 2. A general view of DE-CtT

view in usual thinner than 1 mm, and, what is more important, considerably reduces the amount of scattered radiation with beneficent influence on the image spatial resolution.

The continuous interest on the past climatic changes as well as on the evolution of the ocean basins has determined a steady development coring techniques, including multiple on-situ analysis, among them CT playing an important role [23]. For this reason and by taking into account the existence of a full operational R/V mare Nigrum (R/V Mare Nigrum belongs to the National Institute of Marine Geology and Geoecology – Bucharest), we have taken the decision to built an on-board dual energy CtT designed to generate both dual-energy CT images and digital radiographies. For that reason, this paper will be devoted to the presentation of the main performances of this instrument.

2. Materials and Methods

2.1 DE-CtT

Since sediment (consolidated and unconsolidated) cores was the main object of CT as well as DR investigation, we have chosen a vertical axis multiple detector system. Accordingly, and by taking into account the on-board laboratory size the CtT can

perform dual-enery investigations of core segments with a length of maximum 1 m and a maximum diameter of 12 cm. Because the maximum anodic potential of 160 kV allows investigation of any object with a maximum diameter of 15 cm, this CtT can be successfully used to investigate any geologic sample that fits maximum reconstruction area, *i.e.* 12-14 cm. A general picture of this CtT is reproduced in figure 2.

The dual-enery detection system consists of two times 512 individual solid state X-ray detectors separated by a 1 mm copper shield (Figure 1) that allows a maximum spatial resolution of about 0.5 mm. The reconstruction algorithms consists of an optimized version of Sheep-Logan filtered back projection. A set of five standard samples with well known densities and chemical compositions were used to calculate for each voxel, starting from the reconstructed CT images obtained from each set of detectors, the corresponding values of densities and Z_{eff}. In these conditions, finals CT images were obtained for each chosen section in less than 5 s.

As it has been sated earlier, the same CtT was designed to generate digital radiographies of investigated core, by shifting the core in the between X-ray generator and detectors with a speed of 1m/min. Because both X-ray tube and detectors was shielded with two optically aligned 1 mm lead collimators, the amount of scattered radiation at detectors level was significantly reduced which generated digital radiographies with reduced blur. By using the same standard samples and a personal algorithm we have been able to generate, starting from the low and high energy DR images two new images representing density as well as Z_{eff} radiographs. Additionally, for a better interpretation of these DE-CT images, for each of them, the corresponding histograms were computed and displayed.

The possibility to use the same instrument as CtT and DR device increased significantly the quality of information regarding sediment cores, as after being collected, a core first of all were examined in DR mode and than, the most representative sections were thorough investigated in DE-CT mode.

2.2 Cores

To check the performances of this CtT we have investigate seven cores collected from Danube River, Danube Delta and Black Sea Continental Platform together with a standard one consisting of five sections made from sand with calibrated granularity. Depending on the collecting point, core diameter varied between seven and 12 cm.

It is worth to mention that the Black Sea cores were collected from two different depths (40 and 600 m respectively) as so to investigate both oxygenated and anoxic zones of Continental Shelf.

3. Results and Discussion

The result of our investigation by using proper CtT had two main purposes *i.e.* to estimate the actual instrument performances and to get first results concerning Black Sea Continental Platform sediments.

Instrument performances were better determined by means of three set of standard sample: a set of six materials with known chemical composition and densities (Polyamide 12, Polyetherimide, Polyoxymethylene, Graphite, Teflon and Polyphenylene-sulphide), the last one playing the role of unknown sample, a synthetic core composed of five different sand layers, each with well calibrated granularity, and a

Table 1 Numerical values of low and high energy LAC (in cm^{-1}), densities and Z_{eff} for all six standard sample, the last one (polyphenylenesulphide) being considered as unknown.

Material	μ_l	μ_h	ρ	ρ_{DECAT}	Z_{eff}	$Z_{eff\,DECAT}$
Polyamide 12	0.0926	0.0813	1.016	-	6.158	-
Polyetherimide	0.1121	0.0968	1.274	-	6.400	-
Polyoxymethylene	0.1415	0.1180	1.493	-	7.120	-
Graphite	0.1519	0.1325	1.797	-	6.00	-
Teflon	0.1970	0.1580	2.171	-	8.469	-
Polyphenylene-sulphide	**0.2113**	**0.1436**	**1.620**	**1.630 ±0.064**	**11.1708**	**11.47 ± 0.34**

rectangular matrix of copper strips with gradually decreasing thicknesses, the thinner one being of about 0.5 mm.

As it results from reproduced data, both densities and Z_{eff} of the Polyphenylene-sulphide sample as experimentally determined by means of our CE-CtT differ by the correct ones by about 0.6 % and respectively 2.6 %.

In the case of synthetic core, in Figure 3 we have reproduced one DR and three DE-CT images, the last ones representing LAC distribution as generated by front detectors, density as well as Z_{eff} distribution for two different sections, with different granulation.

By analysing these images it can be remarked first of all that all layers that compose the standard core are well represented on the DR image (right) as well as on the LAC representations. At the same time the granulation of the lower layer is better
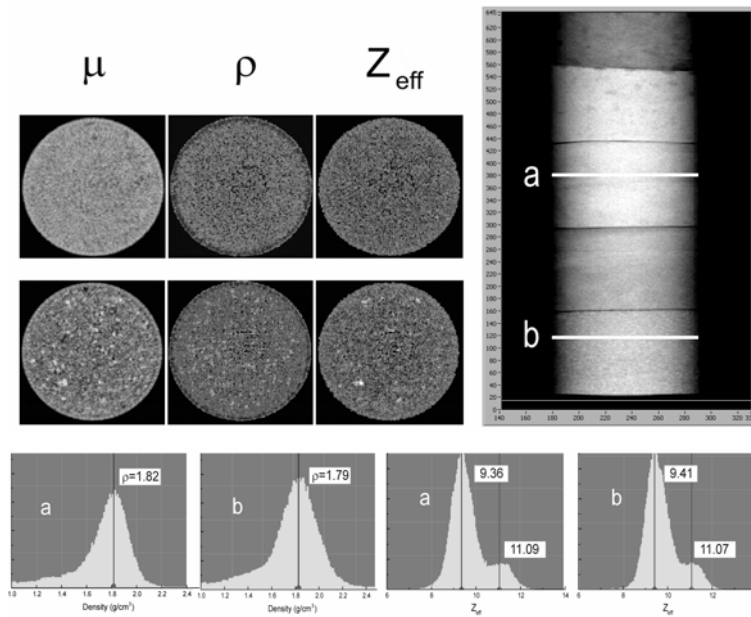

Figure 3. Six DE-CT images (upper, left) illustrating the low energy tomographies (μ), densities (ρ) as well as Z_{eff} distributions corresponding to sections *a* and *b* of DR image of a standard core (upper right) while the lower images represents both densities and Zeff histograms of corresponding sections.

represented, due to the fact that the main size of sand particle is about 0.4 mm, *i.e.* the inferior limit of instrument resolution.

On the inferior row of CT images on both LAC and Z_{eff} few lighter spots could be remarked, spots that are almost invisible on density CT image. In our opinion, these spots represent calcite grains, whose density is very close to quartz that composes sand, but having a higher effective atomic number appear in different hues.

By analyzing CT images histograms a slightly variation in densities between two layers can be remarked, the coarser one presenting a slightly lower density while the effective atomic number appears to be a little higher, probably due to calcite presence. At the same time, on both Z_{eff} images a less intense second peak appears, indicating the presence of a second phase, most probable an argillaceous one. The presence of this second peak confirm previous observations concerning a better phase separation on Z_{eff} images and subsequently on corresponding histogram [24,25].

What concerning the grid use to determine the spatial resolution in DR mode, the best represented was the vertical, 0.5 mm thickness grid, compatible with the thickness of individual detectors, while the horizontal ones, compatible with the X-ray fan beam thickness, was those about 1 mm.

The final test of this DE-CtT was performed by investigating ten cores collected from diverse locations on both Danube River system and Black Sea Continental Platform. The most representative images are reproduced in Figure 5 and 6 (river bed and lacustrine cores) and Figure 7 (continental platform cores).

The images reproduced in Figure 5 shows with clarity the presence of two different sections, one consisting of relatively fine and undisturbed sediments on the superior part of core and the second one an the core bottom containing sediments with different densities organized in inclined laminae, the most probable resulting from turbulent flow, a typical situation for Danube river characterized by a seasonal variation of debit.

It must be pointed out that the observed variation in LAC as it results from both DR image and LAC tomographies are mainly due to a variation of sediment granularity as density CT image shows (an image histogram with three different maxima) rather to sediment composition as Z_{eff} image indicate (only two maxima), most probably, as in the case of standard core due to the presence of clay.

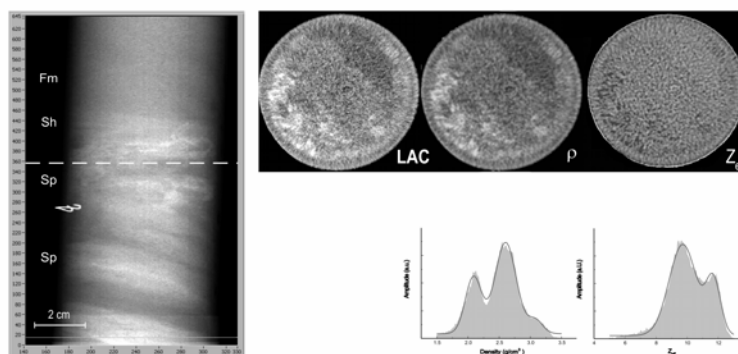Since cores are almost perfect cylindric objects, a considerable amount of

Figure 5 DR and DCT images of a core containing unconsolidated sediments collected from the Danube River bed near at confluence with Danube-Black Sea Channel near Cernavoda town. While density CT image attest the presence of three different components (most probably quartz sand with different granulation as well as clay), the Z_{eff} image present only two maxima corresponding to quartz and another clay mineral component.

information can be obtained directly by observing DR images, as Figure 6 and 7 illustrate.

DR images reproduced in Figure 6 are illustrative for the variety of lithofacieses formed at the contact between the fresh water of Danube River and marine water of the Black Sea. Depending on the local particularities, bottom sediments can contain a considerable amount of organic material inclusive fragments of vegetation that confer a lower capacity of absorption of X ray (left image) or, by contrary contain considerable amount of heavy minerals such as rutile or zircon whose presence, due to an increased absorption, is very well marked on radiography (central image). On the same figure, the right image represents an intermediate situation characterized by the presence of organic debris visible as darker spots due to a reduced absorption dispersed in a mode dense and component consisting of mineral material, also organized in laminae with various thickness and orientation, typical for a turbulent flow.

As expected, the Black Sea Continental Platform sediments presented different in accordance with the depth where they were collected (Figure 7). The difference between two lithofacieses is remarkable. While the low depth sediments collected from the oxygenated zone contain a considerable amount of mussel debris, typical for the *Mytilus* facies existing in this area, the 600 m depth sediments consist entirely of an alternation of undisturbed horizontal fine laminae, slightly tilted, indicating a completely lack of bioturbation as well the presence of a weal bottom current. At a careful examination we
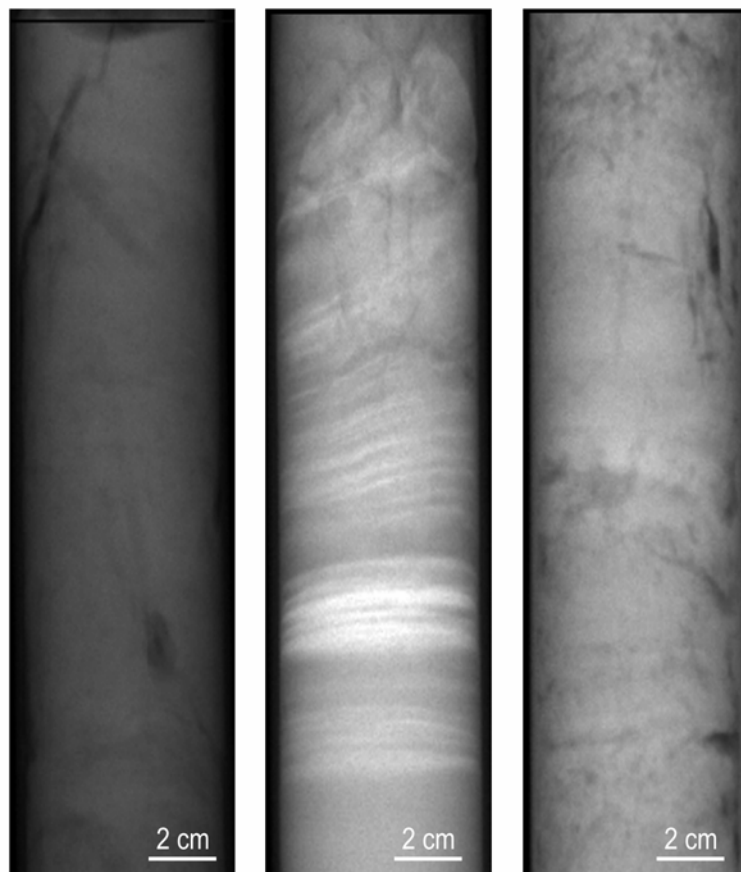

Figure 6 DR of the three cores collected from the Danube Delta (Sulina Channel mouth) illustrating the great variety of lithofacieses characteristic for this region. The planar cross bedded laminae observed on the inferior part of the middle core represents highly mineralized sediments while the dark hues of the first core indicates a reduced absorption most probably due the presence of
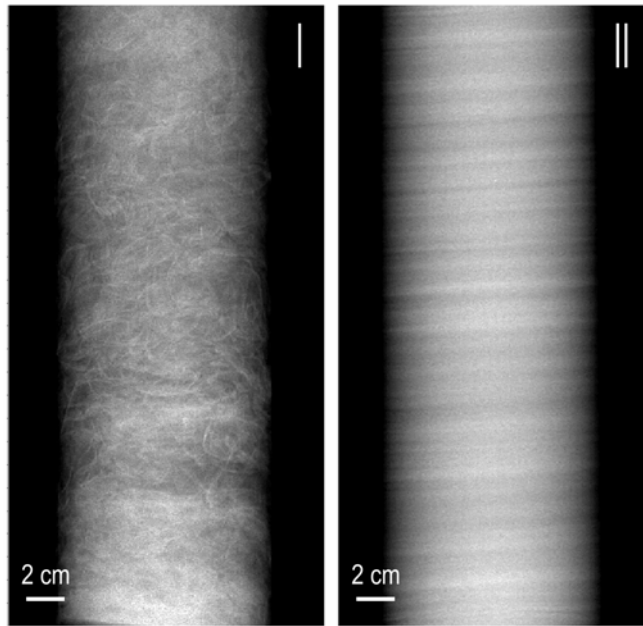
Figure 7 DR images of two cores collected from the Black Sea Continental Platform from an oxygenated zone at a depth of 40 m (left) and from the anoxic zone at 600 m depth (right). While the core collected from an oxygenated zone consist of an alternation of horizontal bedded sand and mussel debris the core collected at 600 m depth contains only almost horizontal fine laminae, specific for the anoxic zone of the Black Sea where the bioturbation is absent.

contend about 254 laminae, but in the absence of a detailed microscopic examination we could not affirm that these are annual or multiannual laminae.

Irrespective of this last remark, all DR images could be considered as significant for the investigated areas.

4. Concluding Remarks

A dual energy X-ray computer tomograph planned to work on-board of R/V mare Nigrum was built and commissioned. By using a single anodic potential X-ray tube and two sets of appropriate detectors separated by a copper shield, this instrument can generate two different tomographies depicting density and respectively effective atomic number distribution for each section of investigated object. Designed for objects with maximum diameter of 12 cm, this tomograph can be used not only to investigate unconsolidated sediments cores but also to study any geological sample that fit into reconstruction area. The same instrument can by successfully used to generate high quality parallax free digital radiographies of the same object, both in density of effective atomic number modes. In all cases, the spatial resolution was about 0.5 mm while the relative errors in determining local values of density as well as effective atomic numbers was no greater than 3.5 %, both parameters attesting the real performances of this instrument.

References

1. R.E. Dodge, J. R. Vaisnys, 'Skeletal growth chronologies of recent and fossil corals'., In: Skeletal growth of aquatic organisms (eds. D.C. Rhoads and R.A. Lutz), Plenum Press, New York, pp. 615-618, 1980

2. A.M. Petrovici, J. E. Siebert, P.E. Lieke, 'Soil bulk density analysis in three dimensions by computer tomographic scanning', Soil Science Society of America Journal, 46, pp 445–450, 1982.

3. V.Cromwell, D.J. Kortum, D.J. Bradley, 'The use of a medical computer tomography (ct) system to observe multiphase flow in porous media', Society of Petroleum Engineers, Paper # 13098 presented at the 59th Annual Technical Conference and Exhibition, September 16-19, Houston, Texas, 1984.

4. H. Vinegar, 'X-ray CT and NMR imaging of rocks', Journal of Petroleum Technology, 38, pp 257–259, 1986.

5. S.L. Wellington, H.J. Vinegar, 'X-ray computerized tomography', Journal of Petroleum Technology 39, pp 885–898, 1987.

6. J.A.M. Kentner, Applications of computerized tomography in sedimentology. Marine Geotechnology, 8, pp 201–211, 1989.

7. W.D. Carlson, C. Denison, 'Mechanisms of porphyroblast crystallization: results from high-resolution computed X-ray tomography', Science, 257, pp 1236–1239, 1992.

8. J.L. Ackerman, W.A. Ellingson, 'Advanced Tomographic Imaging Methods for the Analysis of Materials', Materials Research Society, Pittsburgh, 218 pp, 1991.

9. P. Reimers, J. Goebels, H.-P. Weise, K. Wilding, 'Some aspects of industrial non-destructive evaluation by X- and γ-ray computed tomography', Nuclear Instruments and Methods in Physics Research, 221, pp 201–206, 1984.

10. D. Toye, M. Crine, M. Marchot, 'Imaging of liquid distribution in reactive distillation packings with a new high energy x-ray tomograph', Measurements Science and Technology 16, pp 2213-2220, 2005.

11. A. Hirakimoto, 'Microfocus X-ray computed tomography and it's industrial applications', Analytical Sciences, 17 (suppl.) pp I123-I125, 2001.

12. A.C. Kak, M. Slaney, 'Principles of Computerized Tomographic Imaging', IEEE Press, New York, 322 pp, 1999.

13. G.T. Herman, 'Image reconstruction from projections. The Fundamentals of Computerized Tomography', Academic Press, New York, 231 pp, 1980.

14. W.A., Kalender, 'Computed Tomography: Fundamentals, System Technology, Image Quality, Applications', MCD, Munich, 274 pp, 2001.

15. L. A. Feldkamp, L.C. Davis, J. W. Kress, 'Practical cone-beam algorithm', Journal of the Optical Society of America 1, 612-619, 1984.

16. K. Siegbahn, 'Alpha, beta and gamma ray spectroscopy', North Holland, Amsterdam, 877 pp, 1968.

17. C. Rizescu, C. Besliu, A. Jipa, 'Determination of local density and effective atomic number by the dual-energy computerizet tomography method with the 192Ir radioisotope', Nuclear Instruments and Methods in Physics Research A. 465, 584-599, 2001.

18. L.A.G. Aylmore, 'Use of computer assisted tomography in studying water movement around plant roots', Advances in Agronomy, 49, 1-54, 1993.

19. H. Rogasik, J. W. Crawford, O. Wendroth, I.M. Young, M. Joschko, K. Ritz, 'Discrimination of soil phases by dual energy X-ray tomography', Soil Science Society of America Journal, 63, 741-751, 1999.
20. M. Van Geet, R. Swennen, M. Wevers, 'Towards 3-D petrography.: aplication of microfocus computer tomography in geological science', Computers & Geosciences 27, 1091-1099, 2001.
21. O.G., Duliu, C.T. Rizescu, C. Ricman, 'Dual energy gamma-ray axial computer tomography investigation of some metamorphic and sedimentary rocks', Neues Jahrbuch für Geologie und Paläontolgie 228, 343-362, 2003.
22. T.J. Algeo, M. Phillips, J. Jaminski, M. Fenwieck, 'High Resolution X-radiography of Laminated Sediment Cores', Journal of Sedimentary Research A64, 665 – 668, 1994.
23. B.M. Freifield, T.J. Kneafsey, F.R. Rack, 'On-site geological core analysis using a portable X-ray computed tomographic system', in R.G. Rothwell (ed.), New Techniques in Sediment Core Analysis, Geological Society, London, Special Publication, 267, 165-178, 2006.
24. C.T. Rizescu, G.N. Georgescu, O.G. Duliu, 'High density mineral inclusions in rocks evidenced by gamma-ray tomodensitometry', Journal of Trace and Microprobe Techniques 19, 119-129, 2001.
25. C.T. Rizescu, G.N. Georgescu, O.G. Duliu, S.A. Szobotka, '3-D dual gamma-ray computer axial tomography investigation of polymetallic nodules', Deep Sea Research I, 48, 2529-2540, 2001.